

from preferred wall orientations resulting from the incompatible shear systems associated with orthogonal domain families (Fig. 6).

Regarding the mechanism responsible for generating the optical contrast, we believe that the electric fields associated with the emergent spontaneous polarization must play an important role in modulating the thickness of the deposited solid film. We believe that during the etching process, which proceeds at different rates on the differently charged domain surfaces, a thin coherent insoluble film of  $GdF_3$  is built up. It appears to be this lower index film which is responsible for the interference colours. Ion scattering spectroscopy gives clear indication of gadolinium and fluorine in the coloured surface, with no evidence of oxygen or molybdenum. These peaks, however, do become apparent after ion-milling off the modified surface region.

$GdF_3$  is inferred as the most probable film material since it is almost insoluble in weak HF. The very large index difference between the fluoride and the molybdate appear to be responsible for the bright surface colours. Interesting dielectric and elastic effects occur in the coated crystals, these and a more detailed physical and chemical description of the films will be published shortly.

In conclusion, this technique is fast, very simple, has high resolution and can be repeated

many times on the same surface. So far it has only been used with GMO, but may have applications in other non-water soluble ferroelectrics.

## References

1. T. MITSU and J. FURUICHI, *Phys. Rev.* **90** (1953) 193.
2. M. TANAKA and G. HONJO, *J. Phys. Soc. Japan* **19** (1964) 954.
3. G. V. SPIVAK, E. IGRAS and I. S. ZHELUDEV, *Doklady Akad. Nauk S.S.S.R.* **122** (1958) 54; *Kristallografiya* **4** (1959) 123; *Sov. Phys.-Crystallogr.* **4** (1959) 115.
4. H. BLANK and S. AMELINCKX, *Appl. Phys. Lett.* **2** (1963) 140.
5. J. A. HOOTON and W. J. MERZ, *Phys. Rev.* **98** (1955) 409.
6. J. FOUSEK, M. SAFRANKOVA and J. KACZER, *Appl. Phys. Lett.* **8** (1966) 192.
7. G. L. PEARSON and W. L. FELDMAN, *J. Phys. Chem. Solids* **9** (1959) 28.
8. Y. FURUHATA and K. TORIYAMA, *Appl. Phys. Lett.* **23** (1973) 361.
9. N. NIZEKI and M. HASEGAWA, *J. Phys. Soc. Japan* **19** (1964) 550.

Received 28 January

and accepted 24 February 1977.

A. BHALLA,  
L. E. CROSS

The Pennsylvania State University,  
Materials Research Laboratory,  
University Park,  
Pennsylvania, USA

## The fabrication of the translucent ZnO by sintering

Zinc oxide is a structure-sensitive material with a wurtzite structure. It is not sintered without introducing colour centres; specimens treated at high temperature are yellow. Small amounts of additives such as  $Li^{+1}$  and  $Al^{+3}$  ions result in red and green colourations, respectively [1]. Sintering at temperatures higher than  $1300^{\circ}C$  is not possible because of the high vapour pressure [2]. The fabrication of high-density zinc oxide without colour centres has not been previously reported. This short communication discusses the sintering of zinc oxide treated by  $H_3PO_4$ , which produces white translucent compacts.

Reagent grade basic zinc carbonate was decomposed *in vacuo* at  $300^{\circ}C$  for 30 h. The resultant zinc oxide was added to a solution of a known quantity of reagent grade  $H_3PO_4$ , and the suspension evaporated dry with a heater. The powder was lightly ground and fired at  $500^{\circ}C$  for 24 h in air. Additives amounted to 1.0 at.%. Electron micrographs showed that the particle size of the powder was less than  $0.2\mu m$ . The density of compacts before sintering was about 55% of the theoretical. All the sintering runs were carried out in air at 1000 to  $1250^{\circ}C$ . The zinc oxides sintered at 1000 to  $1200^{\circ}C$  were white, while that at  $1250^{\circ}C$  was slight greenish yellow.

Photomicrographs of sintered sample, Fig. 1, indicate that rapid grain growth occurred in the

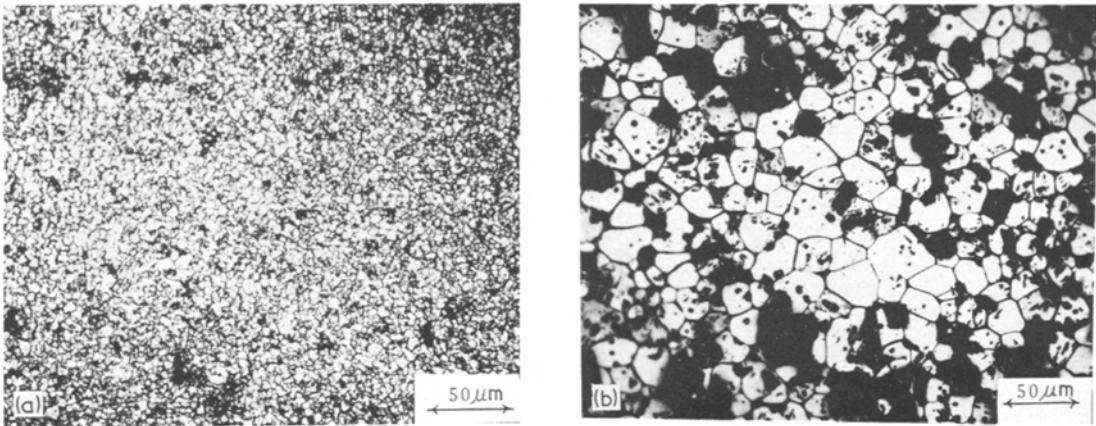


Figure 1 Photomicrographs of ZnO sintered at 1200° C with H<sub>3</sub>PO<sub>4</sub> as an additive; (a) 1 min, (b) 3 h, (c) 50 h.

zinc oxide with H<sub>3</sub>PO<sub>4</sub> as an additive. The density in Fig. 1c is 98% of the theoretical, and the compacts are translucent, as shown in Fig. 2. Obviously from Fig. 1c, small closed pores exist in the grains. If we could eliminate these closed pores, transparent compacts of zinc oxide might be obtained.

According to the phase diagram, ZnO–P<sub>2</sub>O<sub>5</sub> system [3], liquid phase sintering is probable, however, differential thermal analysis yielded no data to show liquid phase was present. The results of X-ray analysis indicated no changes in lattice parameter, therefore we have no information relating to the formation of solid solutions of P<sub>2</sub>O<sub>5</sub>

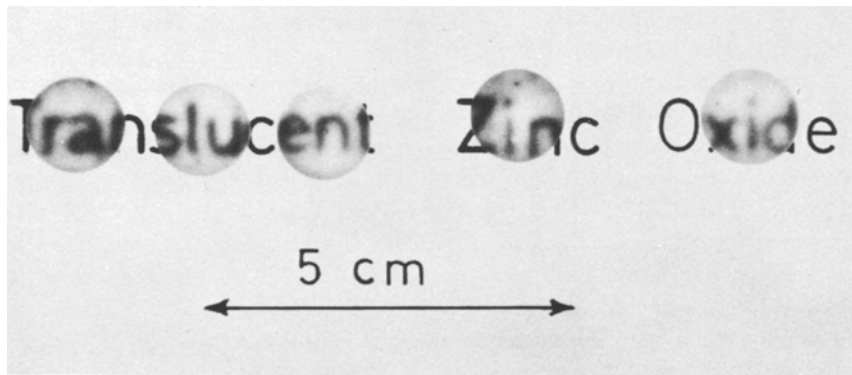
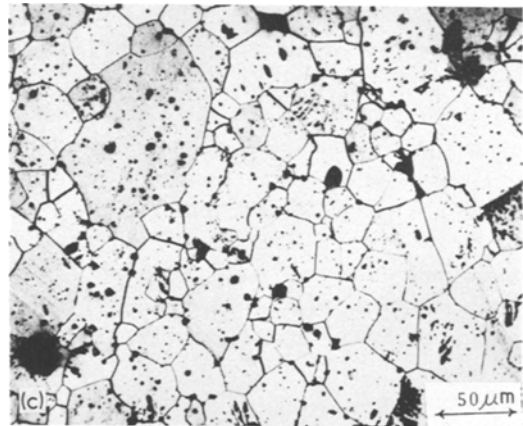
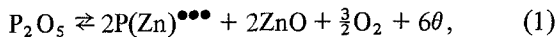
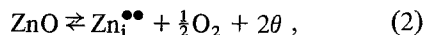


Figure 2 Translucent ZnO sintered at 1200° C for 50 h. Thickness of compacts is about 1 mm.

with zinc oxide. If  $P^{+5}$  ions replace  $Zn^{+2}$  ions on normal lattice sites, the equilibrium reaction is given by the relation



where  $P(Zn)^{\bullet\bullet\bullet}$  is a  $P^{+5}$  ion substituting for a  $Zn^{+2}$  ion on normal lattice sites. The extra semi-free electrons will change the concentration of interstitial zinc ions  $Zn_i^{\bullet\bullet}$  at the equilibrium relation [4]



in the direction of decreasing concentration of interstitial zinc ions. This disagrees with the explanation in which material transport of zinc oxide is controlled by the interstitial zinc ions [5–8]. If  $P^{-3}$  ions substitute for oxygen ions on normal lattice sites, in order to maintain electrical neutrality, oxygen vacancies must be created. Consequently, oxygen diffusion might be enhanced by the addition of  $H_3PO_4$ , but this is not yet established clearly. Further work on the role of  $H_3PO_4$  in the sintering of ZnO is being carried out.

### References

1. W. KOMATSU, M. MIYAMOTO, S. FUJITA, and Y. MORIYOSHI, *Yogyo Kyokai Shi* 76 (1968) 407.
2. H. SCHÄFFER and H. MAYWALD, *Z. Phys. Chem.* B244 (1970) 289.
3. F. L. KATOMACK and F. A. HUNMMEL, *J. Electrochem. Soc.* 105 (1958) 132.
4. K. HAUFFE and J. BLOCK, *Z. Phys. Chem.* 196 (1950) 438.
5. T. J. GRAY, *J. Amer. Ceram. Soc.* 37 (1954) 534.
6. V. J. LEE and G. PARRAVANO, *J. Appl. Phys.* 30 (1959) 1735.
7. W. KOMATSU, Y. MORIYOSHI and N. SETO, *Yogyo Kyokai Shi*, 77 (1969) 347.
8. Y. MORIYOSHI and W. KOMATSU, *J. Amer. Ceram. Soc.* 53 (1970) 671.

Received 25 February  
and accepted 4 April 1977.

YUSUKE MORIYOSHI  
MITSUMASA ISOBE  
YASUSHI HASEGAWA  
*National Institute for Researches  
in Inorganic Materials,*  
WAZO KOMATSU  
*Tokyo Institute of Technology,*  
Tokyo, Japan

### Comments on "fracture measurements on cement paste"

Higgins and Bailey show in their interesting paper [1], that the apparent fracture toughness for paste, mortar and concrete in the ordinary three-point bending test depends on the beam depth. They also in general terms discuss a model explaining this effect, a so called "tied crack model". By this they imply that there exists a residual attractive force between the two faces of a newly formed crack.

Similar thoughts are presented in [2]. The main idea of the model proposed in that paper is to choose the variation of stress  $\sigma$  with crack width  $w$  so that

$$\int_0^{w_1} \sigma dw = G_c \quad (1)$$

$w_1$  representing the crack width where the stress has fallen to zero. This means that the energy

Figure 1 Test results of  $K'_{IC}$  versus specimen depth [1] compared to theoretical curves according to the model proposed in [2].

